Benzene, coronene, and circumcoronene adsorbed on gold, and a gold cluster adsorbed on graphene: Structural and electronic properties

Paulo V. C. Medeiros,* G. K. Gueorguiev, and S. Stafström
Department of Physics, Chemistry and Biology (IFM), Linköping University, SE 581-83 Linköping, Sweden
(Received 25 January 2012; published 14 May 2012)

Density functional theory (DFT) calculations were performed in order to investigate the stability and the electronic structure of graphene-gold interfaces. Two configurations were studied: a gold cluster interacting with graphene and different polycyclic aromatic hydrocarbon (PAH) molecules, namely, C_6H_6 (benzene), $C_{24}H_{12}$ (coronene), and $C_{54}H_{18}$ (circumcoronene) adsorbed on an Au(111) surface. Nonlocal interactions were accounted for by using the semiempirical DFT-D2 method of Grimme. A limited set of calculations were also performed by using the first-principles van der Waals density functional method (vdW-DF). Adsorption distances around 3 Å and electronic charge transfer values of about (3–13) $\times$ $10^{-3}e^-$ per carbon atom were predicted for all systems. No major changes resulting from the adsorption of the gold cluster were detected in the graphene's density of states. The DFT-D2 results involving the adsorption of the PAH molecules on gold show an estimated binding energy of 73 meV per carbon atom, as well as an electronic charge loss of 0.10×10^{-2} e^-, also per carbon atom, for an extended graphene sheet adsorbed on a gold surface. The modeling of the adsorption of C_6H_6 molecule on a gold surface suggests that the vdW-DF method provides more accurate results for the binding energies of such systems, in comparison to pure DFT calculations, which do not take the nonlocal interactions into account, as well as to simulations employing the DFT-D2 method.

DOI: 10.1103/PhysRevB.85.205423 PACS number(s): 73.40.Ns, 68.43.−h, 31.15.es

I. INTRODUCTION

The novel electronic and mechanical properties of graphene have been extensively studied after a method for obtaining free-standing graphene was presented in 2004.[1] Graphene is considered, among several other applications, as a prominent candidate for future electronic and optoelectronic applications.[2] This has motivated studies of transport properties and possible ways to modify graphene in order to acquire semiconducting properties. Changes in graphene properties induced by the interaction with different molecules, clusters, or even single atoms[3–6] have been investigated in detail. Within this context and since the development of graphene-based devices also requires graphene-metal contacts,[7] the knowledge of the underlying physics for graphene-metal systems has recently attracted much research interest.

Properties such as charge transfer,[8,9] contact resistance, and electron transport[10,11] are considerably affected by the interactions at the graphene/metal interface. Giovannetti *et al.*[9] found, by employing DFT local-spin-density-approximation (LSDA) calculations, that the interactions in metal-graphene systems can occur either by chemisorption, as they have reported for Co, Ni, and Pd (the graphene's electronic bands being considerably disturbed), or through weak physisorption bonding, as in the case of Al, Cu, Ag, Au, and Pt. For the metals belonging to the latter group, the contacts result in doping (charge transfer) of graphene but with only minor changes on its electronic structure. In fact, it has been experimentally demonstrated that a *p*-type doping, with almost no changes in the graphene bands, occurs when a sheet of graphene is adsorbed on a gold substrate.[8] Such a configuration represents significant technological interest, due to the low reactivity and high stability at relatively high temperatures of gold: a frequently desired material for electronic contacts and components.

A different approach to the metal-graphene interactions was recently adopted by Vanin *et al.*[12] Through an analysis employing the van der Waals density functional (vdW-DF),[13,14] the authors have found that all the considered metal surfaces bind weakly to graphene (instead of being categorized into two different groups according to the kind of the interaction with graphene: strong and weak). Their results, however, are not in agreement with previously reported experimental results, which indicate that the interaction between graphene and the metals Ni (Refs. 15 and 16) and Co (Ref. 17) cannot be regarded as being weak. On the other hand, Vanin *et al.*[12] have also shown that the graphene-metal bonding predicted by local-density approximation (LDA) calculations, in the case of the metals belonging to the physisorption group, results, at least in part, from the exchange term of the LDA exchange-correlation (*xc*) functional. Although the LDA calculations in Ref. 9 reproduce well the results of experimental measurements on related systems, the above-mentioned exchange-induced physisorption is contradictory with the nonlocal character of the van der Waals interactions, which are expected to play a considerable role in such systems.

In this work, first-principles density functional theory (DFT) calculations are performed in order to address the stability and the electronic structure of a gold cluster with 49 atoms adsorbed on a graphene sheet, as well as of three polycyclic aromatic hydrocarbon (PAH) molecules: C_6H_6 (benzene), $C_{24}H_{12}$ (coronene), and $C_{54}H_{18}$ (circumcoronene), adsorbed on an Au(111) surface. Besides employing the local exchange and correlation functionals,[18] also nonlocal dispersive interactions are accounted for by employing the semiempirical DFT-D2 method of Grimme[19] or the first-principles vdW-DF functional of Dion *et al.*[13]

II. COMPUTATIONAL METHODS

The DFT simulations carried out in this work use the numerical implementation of the VASP program,[20] making

use of projector augmented-wave (PAW) potentials.[21,22] The generalized gradient approximation (GGA) was adopted, with exchange and correlation functionals according to the approach proposed by Perdew, Burke, and Ernzerhof (PBE).[18] All plane waves corresponding to kinetic energies up to 700 eV were included in the basis set. The Brillouin zones were sampled by using the Monkhorst-Pack methodology with gamma point-centered $3 \times 3 \times 1$ grids for relaxations and $5 \times 5 \times 1$ grids for the total energy and density-of-states (DOS) calculations. Partial occupancies of electronic states were set according to different methods, depending on a given task: for relaxations involving gold atoms only, the Methfessel-Paxton method of order 2 with a smearing width of 0.2 eV was used, while a Gaussian smearing with a width of 0.05 eV was adopted throughout the relaxations of all the composed systems. Finally, the tetrahedron method with Blöchl corrections was employed when calculating all total energies and DOS.

Two different methods, which included dispersion corrections, were employed throughout the simulations: (i) the first-principles vdW-DF, developed by Dion *et al.*,[13] and implemented in VASP by Gulans, Puska, and Nieminen;[23] and (ii) the semiempirical DFT-D2 method of Grimme.[19] For the DFT-D2 calculations, we used the parameters suggested in Ref. 24, namely, 40.62 J nm^6/mol for the dispersion coefficient (C_6), and 1.772 Å for the vdW radius (R_0) for gold. The dispersion coefficient and vdW radius values adopted for carbon and hydrogen were the ones suggested by Grimme in the original discussion of his method.[19] We set the global scaling factor s_6 to the value of 0.75, which was determined in Grimme's work for calculations employing the PBE functional. The cutoff radius for pair interactions employed in the empirical dispersion correction is 12 Å, except for the simulations involving the $C_{54}H_{18}$-Au(111) model system, in which, in order to avoid spurious interactions between neighboring images of the $C_{54}H_{18}$ molecule, a cutoff radius of 8 Å was applied. We checked the consistency of these parameters by calculating the Au(111) surface energy and the cohesive energy for the bulk phase of a gold slab. The energy values we have obtained read 1.46 J/m^2 (0.091 eV/Å^2) and 3.69 eV/atom, exhibiting an excellent agreement with the values of 1.50 J/m^2 (Ref. 25) and 3.81 eV/atom (Ref. 26) obtained in experimental measurements for the same energy features.

The binding energies were calculated as

$$E_{b1} = -\left(E_{coh}^{\mathrm{Au_{49}/graphene}} - E_{\mathrm{coh}}^{\mathrm{Au_{49}}} - E_{\mathrm{coh}}^{\mathrm{graphene}}\right), \quad (1)$$

$$E_{b2} = -\left(E_{\mathrm{coh}}^{\mathrm{PAH/Au(111)}} - E_{\mathrm{coh}}^{\mathrm{PAH}} - E_{\mathrm{coh}}^{\mathrm{Au(111)}}\right), \quad (2)$$

i.e., for each case the bonding energy corresponds to the difference between the composed system's cohesive energy ($E_{\mathrm{coh}}^{\mathrm{Au_{49}/graphene}}$, $E_{\mathrm{coh}}^{\mathrm{PAH/Au(111)}}$) and the cohesive energies of its isolated building components ($E_{\mathrm{coh}}^{\mathrm{Au_{49}}}$, $E_{\mathrm{coh}}^{\mathrm{graphene}}$, $E_{\mathrm{coh}}^{\mathrm{PAH}}$, $E_{\mathrm{coh}}^{\mathrm{Au(111)}}$). According to such a definition, a positive binding energy value means that bonding is energetically favorable. In order to reduce the possible numerical errors, care was taken to employ supercells with the same shape, i.e., with equal lattice vectors, when obtaining the total energies of each model system and its corresponding isolated components. Spin polarization was not considered. This decision was taken after performing preliminary test calculations in which, for the systems under consideration, no magnetic behavior has been detected. The charge transfers were calculated according to the Bader method[27] as implemented by following the algorithms described in Refs. 28–30.

Periodic boundary conditions were used and dipole corrections were taken into account for both the local potentials and the total energies. In addition, a vacuum length of 20 Å was introduced between neighboring images of the unit cell along the direction perpendicular to the initial surfaces—referred to here as the z direction. The self-consistency cycles were considered as converged when the differences between the values of both the total energies and the Kohn-Sham eigenvalues calculated in two consecutive "electronic steps" were smaller than 10^{-5} eV.

The relaxations of the combined graphene/PAH-gold systems were performed in two steps: first the geometries were optimized using the PBE exchange and correlation functional. These geometries were then taken as starting points for obtaining the new equilibrium distances with the vdW interactions accounted for. During the calculations, which included the vdW interactions, all gold atoms were kept fixed, i.e., their positions were not reoptimized. This approach of keeping the atoms in the metal slab fixed is similar to the one adopted in Refs. 12 and 31 (except that in Ref. 12 the atoms of the different metal slabs are kept fixed to the corresponding experimental lattice parameters). The residual minimization method of direct inversion in the iterative subspace (RMM-DIIS) variable metric algorithm[32] was employed to move selected atoms until the maximal Hellmann–Feynman force[33] acting on them met the criterion of becoming weaker than 5×10^{-2} eV/Å. The unit cell vectors were not allowed to change during the calculations. The equilibrium separations between the system's components are calculated as

$$d_{\mathrm{eq_1}} = |\bar{z}_{\mathrm{Au_{49}}} - \bar{z}_{\mathrm{graphene}}|, \quad (3)$$

$$d_{\mathrm{eq_2}} = |\bar{z}_{\mathrm{PAH}} - \bar{z}_{\mathrm{Au(111)}}|, \quad (4)$$

where $\bar{z}_{\mathrm{Au_{49}}}$ is the z coordinate of the center of mass of the first layer of the Au_{49} cluster (respectively, $\bar{z}_{\mathrm{PAH}}$ corresponds to the z coordinate of the center of the mass of the PAH molecule in the case of the class of systems containing PAH) and $\bar{z}_{\mathrm{graphene}}$ (respectively, $\bar{z}_{\mathrm{Au(111)}}$) is the z coordinate of the center of mass of those atoms in the graphene layer [Au(111) surface] which are located right underneath the Au_{49} cluster (PAH molecule).

III. RESULTS AND DISCUSSION

In Fig. 1, a side view of the relaxed Au_{49}-graphene system is displayed. There are 24, 16, and 9 atoms, respectively, in the

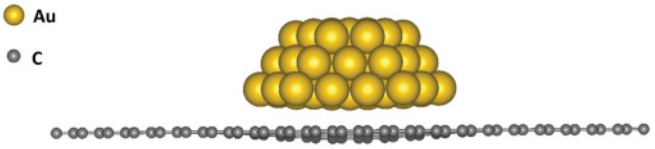

FIG. 1. (Color online) Atomic configuration at equilibrium for the A_{49}-graphene model system.

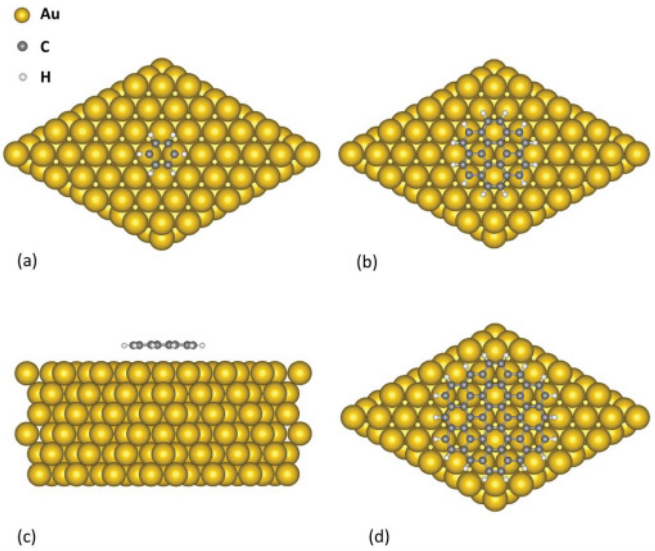

FIG. 2. (Color online) Atomic configurations at equilibrium for the model systems C_6H_6-Au(111) (a), $C_{24}H_{12}$-Au(111) top (b) and side (c) views, and $C_{54}H_{18}$-Au(111) (d). The side view was omitted for the first and last systems, as it is very similar to the one shown in the item (c).

first, second, and third layers of the Au_{49} cluster, which was extracted from a three-layer Au(111) slab. The graphene unit cell was constructed by repeating its two-atom primitive cell 12 times along the direction of each of its lattice vectors. The atomic configurations at equilibrium for the C_6H_6-Au(111), $C_{24}H_{12}$-Au(111), and $C_{54}H_{18}$-Au(111) systems are shown in Figs. 2(a)–2(d). For the set of calculations involving the PAH molecules, the gold surface was represented by a 288-atom slab divided into six layers each containing 48 atoms. The two inner slab layers were kept fixed at the bulk interlayer distance of 2.40 Å (calculated by us at the same level of theory). The slab's structural properties, which were calculated without including the effects of vdW interactions, are in very good agreement with those reported for a similar model system in Ref. 34.

Results relevant to the structural and electronic properties of all systems studied are listed in Tables I and II. In order to simplify the discussion, we have divided this section into two subsections, discussing separately the results obtained by using PBE only and PBE + vdW calculations.

A. Perdew, Burke, and Ernzerhof

For the system in Fig. 1, we obtain an Au_{49}-graphene equilibrium distance of 3.70 Å (Table I), and we predict a *p*-type doping of the graphene sheet, with a net charge transfer of 0.267 e^- estimated by using the Bader method. The number of those carbon atoms at the graphene sheet which are overlapped by the gold cluster, is approximately 76. Taking into account this number, we can estimate the charge transfer per carbon atom in contact with gold as being around 0.0035 e^-. Despite of a shift of -0.24 eV in the graphene's Fermi level with respect to the Dirac point, the partial density of states (PDOS) of the carbon atoms remains similar to the DOS calculated for an isolated graphene layer. It is worth noting, however, that given the use of periodic boundary conditions and the fact that the gold cluster only covers a part of the graphene supercell (approximately 26% of the carbon atoms are overlapped by gold atoms), the shift in the graphene's Fermi level calculated for this model system is expected to be considerably lower than for full coverage.

The equilibrium distances obtained for the systems PAH molecules—gold slab are 3.41 Å (C_6H_6), 3.39 Å ($C_{24}H_{12}$), and 3.50 Å ($C_{54}H_{18}$), respectively. The electronic charge transfers in the case of these model systems are obtained in the same way as described above for the gold cluster model system and are found to be 0.059, 0.135, and 0.162 e^-, for the C_6H_6, $C_{24}H_{12}$, and $C_{54}H_{18}$ molecules, respectively. Normalizing these numbers with the number of carbon atoms involved in the interactions, we obtain 0.0098, 0.0056, and 0.0030 e^- per carbon atom. As will be discussed in the next section, the decreasing of the charge transfer per carbon atom is not primarily a size effect but rather an effect due to the ratio between the number of carbon atoms belonging to the exterior CH groups of the PAH molecule (CH) and those that are bound to other carbon atoms only. The former are considerably more reactive, and they are responsible for a large part of the charge transfer from the PAH molecules. This effect allows us to extrapolate the results for the adsorption of the PAH molecules on gold to an infinite graphene-Au(111) system.

A result perceived as most probably lacking precision is the small binding energies found in the PBE (only) calculations.

TABLE I. Distances between the nearest-neighbor atoms in the isolated components of a model system (d_0), equilibrium separations between the components of a model system (d_{eq}), and interlayer spacing in the Au_{49} cluster and for the Au(111) surface (d_{ij}). The numbering of the layers, in both the gold cluster and the slab, starts by the layer closest to the interface. For each of the vdW calculations (namely, vdW-DF and DFT-D2), the atoms of the Au(111) slab were kept fixed at their geometry obtained by PBE (only). All local correlations were treated according to the PBE parameterization within the GGA approximation. All values are expressed in Å. See main text for details.

		d_{eq}			Interlayer distances		
System	d_0	PBE	vdW-DF	DFT-D2	d_{12}	d_{23}	d_{34}
Graphene	1.43	–	–	–	–	–	–
Au	2.94	–	–	–	2.43	2.39	2.40
Au_{49}-graphene	–	3.70	–	3.05	2.26	2.22	–
C_6H_6-Au	–	3.41	3.22	3.12	2.43	2.38	2.40
$C_{24}H_{12}$-Au	–	3.39	3.27	3.20	2.43	2.38	2.40
$C_{54}H_{18}$-Au	–	3.50	–	3.15	2.42	2.39	2.40

TABLE II. Binding energies (E_b) and electronic charge transfers (ΔQ) per carbon atom on the contact region (N_C) between components of an interface model system. The electronic charge transfer occurs always in the direction from the carbon to the gold.

	E_b/N_C (meV)			$\Delta Q/N_C$ ($\times 10^{-2}$ e$^-$)		
System	PBE	vdW-DF	DFT-D2	PBE	vdW-DF	DFT-D2
Au_{49}-graphene	1.1	–	99.8	0.35	–	0.32
C_6H_6-Au	5.6	99.9	221.3	0.98	1.28	1.67
$C_{24}H_{12}$-Au	− 0.6	94.0	150.4	0.56	0.71	0.88
$C_{54}H_{18}$-Au	− 0.8	–	120.3	0.30	–	0.62

These energies are either negative or of the order of 1 meV per carbon atom. Such negative/small values of binding energies correlates with the well-known fact that, although the GGA approximation is good enough for reasonable structural predictions for systems in which long-range interactions are relevant, it fails to provide a realistic description for the interaction energies. Therefore, it emerges as a necessary sophistication of the simulations to include the dispersive forces between the interface constituents in the modeling.

B. PBE + vdW

The effect, on the equilibrium separations between the interface constituents, of applying the DFT-D2 dispersion correction[19] is a marked reduction of these distances compared to the PBE (only) results. Thus, the Au_{49}-graphene distance decreases from 3.70 to 3.05 Å, while the new equilibrium distances for the three PAH (C_6H_6, $C_{24}H_{12}$, and $C_{54}H_{18}$)-Au(111) systems are 3.12, 3.20, and 3.15 Å, respectively (see Table I). In agreement with the reduction in the distances between the interacting subsystems, there is also the substantial increase in the binding energies. The binding energy of Au_{49} on graphene becomes 100 meV per carbon atom, and for the series of PAH-Au(111) systems, the binding energies per carbon atom become 221, 150, and 120 meV, for C_6H_6, $C_{24}H_{12}$, and $C_{54}H_{18}$ molecules, respectively.

To investigate how the individual carbon atoms contribute to the binding energy between the different PAH molecules and the gold slab (Fig. 2), we have followed the approach of Björk *et al.*[35] This approach highlights the difference in the contributions to the binding energy of a PAH-Au interface between C atoms belonging to the exterior CH groups of the PAH molecule and those that are bound to other carbon atoms only (CC). A linear fit is made to the binding energies per carbon atom relevant to the systems C_6H_6-Au(111), $C_{24}H_{12}$-Au(111), and $C_{54}H_{18}$-Au(111) systems, plotted as a function of the ratio N_H/N_C of the number N_H of hydrogen atoms and the number N_C of carbon atoms in each molecule (see Fig. 3). This fit is remarkably good, and it is therefore relevant to make an extrapolation to systems with a higher CC content. We estimate that the CC contribution (E_{CC}) is approximately 73 meV per carbon atom, while the CH contribution (E_{CH}) is 222 meV per CH group. Thus, the radical CH groups at the circumference of the PAH are much more reactive than the interior CC atoms. The differences between the values obtained for E_{CC} and E_{CH} by us and in Ref. 35 ($E_{CC} = 70$ meV and $E_{CH} = 140$ meV) are not unexpected, since in Ref. 35 the calculation was performed within the vdW-DF scheme, and, in addition, the DFT-D2 method is known to overestimate binding energies of systems with similar characteristics. The fact that the CH radicals interact at least twice as strongly with the gold surface as the individual carbon atoms explains why the $C_{24}H_{12}$ and $C_{54}H_{18}$ molecules became distorted when interacting with the gold slab, with their concavity facing the surface of the metal. The only exception is the C_6H_6 molecule, which, being small enough, keeps its original planar geometry.

The PAH molecules considered here may be seen as prototypic graphene pieces cut out from an infinite graphene sheet and with their dangling bonds passivated with hydrogen atoms. With this picture in mind, the calculations focusing on the different-sized-PAH-Au(111) systems represent consecutive approximations to describing an infinite graphene-Au(111) interface. Such approximations become better as the number of carbon atoms in the PAHs increases. In the limit, an infinite PAH becomes equivalent to a graphene layer. In agreement with this picture, a limit of zero for the N_H/N_C ratio means that the extrapolated value of the CC contribution to the binding energy ($E_{CC} = 73$ meV) is actually the value inherent to graphene: it is the estimated binding energy per carbon atom for a graphene-Au(111) interface. This value is considerably larger than the binding energy of 30 meV per carbon atom for

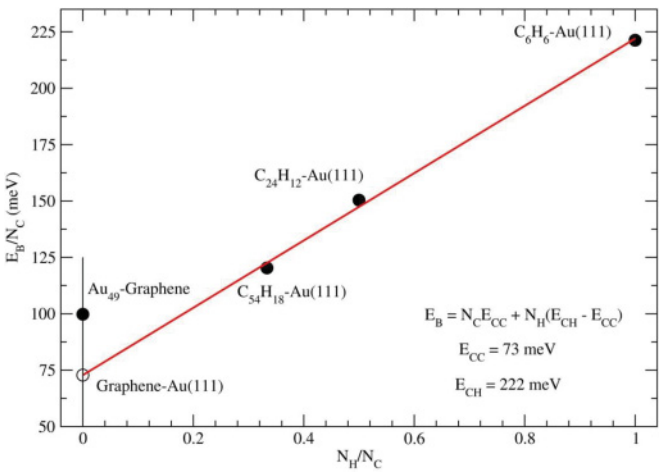

FIG. 3. (Color online) Binding energies per carbon atom plotted as a function of the N_H/N_C ratio for the various model systems. N_H and N_C correspond to the number of hydrogen and carbon atoms, respectively. A linear fit was applied to the energies of the C_6H_6-Au(111), $C_{24}H_{12}$-Au(111), and $C_{54}H_{18}$-Au(111) model systems only. The hollow circle represents the extrapolated binding energy per carbon atom expected for an extended graphene-Au(111) system (E_{CC}). See main text for details.

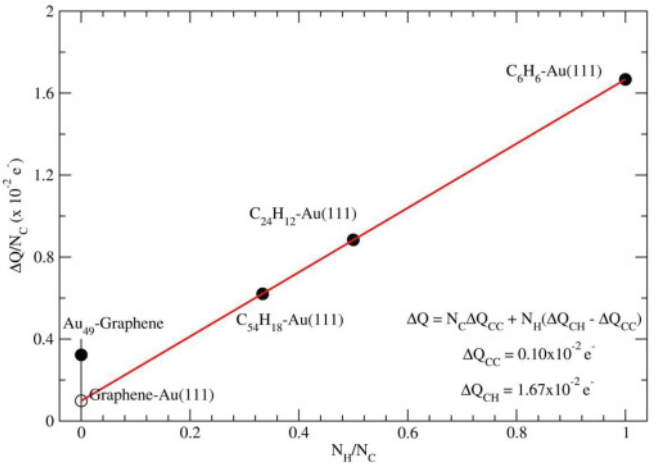

FIG. 4. (Color online) Electronic charge transfer per carbon atom ($\Delta Q/N_H$) from the carbon components to the gold components of the model systems, plotted as a function of the N_H/N_C ratio for the Au_{49}-graphene, C_6H_6-Au(111), $C_{24}H_{12}$-Au(111), and $C_{54}H_{18}$-Au(111) model systems. A linear fit was applied to the charge transfers in the PAH-Au(111) systems only. The hollow circle represents the extrapolated electronic charge transfer per carbon atom expected for an extended graphene-Au(111) system (ΔQ_{CC}). The electronic charge transfer occurs always in the direction from the carbon component to the gold component of the model system.

the graphene-Au(111) interface reported in Ref. 9. However, the binding energy value obtained here, and the one reported in Ref. 9 are not directly comparable, since the results in Ref. 9 were obtained using the LDA approximation with no corrections in the description of dispersive forces. The binding energy per carbon atom of 100 meV calculated for the Au_{49}-graphene system (Fig. 3) is higher than the value predicted for the same quantity in the graphene-Au(111) system, 73 meV, which can be explained by the fact that the gold atoms at the boundary of the cluster are expected to be more reactive than those belonging to a FCC Au(111).

It is illustrative to analyze also the charge transfer between the subsections of the model systems C_6H_6-Au(111), $C_{24}H_{12}$-Au(111), and $C_{54}H_{18}$-Au(111) applying the methodology employed above for the binding energies. In Fig. 4, the amount of electronic charge, per carbon atom, transferred from the graphene sheet and from the three PAH molecules to the respective gold subsections, is plotted as a function of the ratio N_H/N_C. Again, a linear fit has been performed on the values relevant to the PAH-Au(111) systems. From this analysis, the calculated average contribution ΔQ_{CH} of the external CH groups belonging to each PAH molecule to the electronic charge transfer is 1.67×10^{-2} e$^-$. This value is markedly larger than the average contribution ΔQ_{CC} of approximately 0.10×10^{-2} e$^-$, coming from the carbon atoms at internal sites for each PAH molecule. These results are not only consistent with the larger contribution of CH groups to the binding energy discussed above but also provides an explanation for the decreasing amount of charge transfer per carbon atom as the size of the PAH molecule increases. Within the same context as in the analysis of the binding energies, ΔQ_{CC} emerges as an estimate for the average electronic loss per carbon atom for the "case-limit" of an infinite graphene layer adsorbed on an Au(111) surface.

In order to assess the reliability of the results obtained by employing the DFT-D2 method, we performed also a limited set of calculations making use of the computationally more demanding vdW-DF method. The PAH's considered were the C_6H_6 and the $C_{24}H_{12}$ on top of the gold surface. The calculated vdW-DF values for all three characteristics discussed above—the equilibrium distance, the charge transfer, and the binding energy—are between the values for the same characteristics obtained by PBE (only) and by DFT-D2 (Tables I and II). The vdW-DF value for the C_6H_6-Au(111) equilibrium distance is 3.22 Å. The binding energy of 100 meV per carbon atom calculated for the C_6H_6-Au(111) model system compares well to the energy value of 0.55 eV/molecule (91.67 meV per carbon atom) reported in Ref. 31—a study carried out at a similar level of theory. On the other hand, our binding energy is by approximately 38 meV less than the value of 138.4 meV reported in Ref. 35 for the same adsorption configuration of a C_6H_6 molecule on gold [see Fig. 2(a)]. This difference is attributed to the fact that both here and in Ref. 31, the gold atoms were kept fixed in their GGA-PBE equilibrium positions, whereas the geometric structure of the metal slab in Ref. 35 was optimized by using the vdW-DF scheme. Nonetheless, we achieve an excellent agreement with the experimental value of 14.7 kcal mol^{-1} per C_6H_6 molecule (106.2 meV per carbon atom) reported in Ref. 36. However, an important conclusion is that, regardless of the adopted strategy for performing the structural optimizations, the binding energy values obtained in this work for the C_6H_6-Au(111) system, by employing the vdW-DF functional, as well as the binding energy values reported in Refs. 31 and 35 for the same model system (and also calculated by using the vdW-DF functional), compare better to the experimentally measured value reported in Ref. 36 than the binding energy value obtained using the DFT-D2 method. Based on this discussion, we expect that the results reported above from the calculations using the DFT-D2 method to some extent overestimates the binding energies for model systems including PAH molecules interacting with a gold surface.

IV. COMPARATIVE ANALYSIS OF THE RESULTS

Despite of the numerical differences in the results obtained by using the two different van der Waals methods, DFT-D2 and vdW-DF, both methods represent an important improvement over the PBE (only) description of the class of model systems representing graphene-gold interfaces. As illustrated by the results listed in Table II, while the PBE (only) calculations predict either the absence or the formation of extremely weak chemical bonds between the components of the studied systems, both vdW approaches predict binding energy values which are at least one order of magnitude larger. These energy values, however, are still of the order of 100 meV, thus, confirming that the binding in such systems is mostly a result of nonlocal interactions.

No experimental data regarding equilibrium distances in PAH-gold systems as those studied here or similar ones is currently available. Nonetheless, Toyoda *et al.*,[31] by analyzing the differences between their theoretically predicted and experimentally measured values for the work-function

changes in the cases of the model systems C_6H_6-Cu(111), C_6H_6-Ag(111), and C_6H_6-Au(111), have predicted that the values calculated by using the vdW-DF for the molecule-metal equilibrium distances in such systems should be larger than the experimentally measured ones. On the other hand, the DFT-D2 method was found to underestimate (by ∼4–8%) the experimental metal-sulfur distance for a model system consisting in a thiophene molecule (C_4H_4S) adsorbed on a Cu(111) surface.[37] Thus, it is to be expected that the experimentally measurable adsorption distances for the class of PAH-Au(111) model systems have values between the ones estimated here by employing the two vdW methods. The DFT-D2 method provides the largest calculated binding energies and, consistently, the smallest equilibrium distances as well (Table I). The results of our calculations for the C_6H_6-Au(111) model system indicate that among the three methods employed here, the vdW-DF is the most suitable one for the prediction of the energetic properties of graphene-gold interfaces.

V. CONCLUSIONS

DFT calculations were performed to address the structural and electronic properties of the graphene-gold interface. This was done using two different approaches: (i) a gold cluster interacting with an infinite graphene layer, and (ii) three different PAH molecules adsorbed on an infinite Au(111) surface. The description of graphene/PAH-gold interfaces by means of both the DFT-D2 and vdW-DF methods (which account for the van der Waals interactions) represents an important improvement over the description without accounting for the nonlocal interactions, given the fact that the interaction between gold atoms and a large variety of carbon-based nanostructured materials is believed to occur by means of physisorption processes. This is illustrated by the lack of any significant changes in the DOS for graphene when the gold cluster is placed in its close vicinity, in spite of a shift of −0.24 eV detected in its Fermi level. Binding energy values of the order of 100 meV per carbon atom were predicted by using both the vdW methods, in contrast with negligible binding energy values (<6 meV) calculated by employing only the DFT-PBE level of theory. Our results emphasize the vdW-DF as the most suitable approach, among the ones adopted here, for calculating the binding energies of PAH-Au(111) systems. We confirm the previously reported positive linear dependence between the binding energy per carbon atom and the ratio N_H/N_C for PAH molecules adsorbed on a gold surface. This indicates that a carbon atom belonging to the exterior CH-groups of the PAH molecules interacts more strongly with the gold slab than a carbon atom, which is covalently bonded to three other carbon atoms (CC-type carbon atom). In addition, we also find a positive linear dependence between the amount of electronic charge transferred from the PAH to the metal and the ratio N_H/N_C, which is consistent with the behavior displayed by the binding energies and highlights even more the differences between a CC-type carbon atom and a carbon atom belonging to a CH-group. Consequently, we predict for an extended graphene layer adsorbed on an Au(111) surface, at the DFT-D2 level of theory, a binding energy of 73 meV and an electronic charge loss of 0.10×10^{-2} e^-, both per carbon atom. All results presented here for the graphene/PAH-gold models systems at the three levels of theory (PBE, DFT-D2, and vdW-DF) suggest long-range physisorption interactions at the graphene-gold interface.

ACKNOWLEDGMENTS

P.V.C.M. and G.K.G. gratefully acknowledge support by the Swedish Foundation for International Cooperation in Research and Higher Education (STINT) through Project No. YR2009-7017. G.K.G. acknowledges support by Swedish Research Council (VR). The National Supercomputer Center in Linköping (NSC) and the Matter Network of Excellence, Sweden, are gratefully acknowledged for providing high performance computational resources.

*paume@ifm.liu.se

[1] K. S. Novoselov, A. K. Geim, S. V. Morozov, D. Jiang, Y. Zhang, S. V. Dubonos, I. V. Grigorieva, and A. A. Firsov, Science **306**, 666 (2004).

[2] A. K. Geim and K. S. Novoselov, Nat. Mater. **6**, 183 (2006).

[3] M. Amft, B. Sanyal, O. Eriksson, and N. V. Skorodumova, J. Phys.: Condens. Matter **23**, 205301 (2011).

[4] K. T. Chan, J. B. Neaton, and M. L. Cohen, Phys. Rev. B **77**, 235430 (2008).

[5] O. Leenaerts, B. Partoens, and F. M. Peeters, Phys. Rev. B **77**, 125416 (2008).

[6] P. V. C. Medeiros, A. J. S. Mascarenhas, F. de B. Mota, and C. M. C. de Castilho, Nanotechnology **21**, 485701 (2010).

[7] J. Wintterlin and M. L. Bocquet, Surf. Sci. **603**, 1841 (2009).

[8] I. Gierz, C. Riedl, U. Starke, C. R. Ast, and K. Kern, Nano Lett. **8**, 4603 (2008).

[9] G. Giovannetti, P. A. Khomyakov, G. Brocks, V. M. Karpan, J. van den Brink, and P. J. Kelly, Phys. Rev. Lett. **101**, 026803 (2008).

[10] S. Barraza-Lopez, M. Vanevic, M. Kindermann, and M. Y. Chou, Phys. Rev. Lett. **104**, 076807 (2010).

[11] E. J. H. Lee, K. Balasubramanian, R. T. Weitz, M. Burghard, and K. Kern, Nat. Nanotechnol. **3**, 486 (2008).

[12] M. Vanin, J. J. Mortensen, A. K. Kelkkanen, J. M. Garcia-Lastra, K. S. Thygesen, and K. W. Jacobsen, Phys. Rev. B **81**, 081408(R) (2010).

[13] M. Dion, H. Rydberg, E. Schröder, D. C. Langreth, and B. I. Lundqvist, Phys. Rev. Lett. **92**, 246401 (2004).

[14] M. Dion, H. Rydberg, E. Schröder, D. C. Langreth, and B. I. Lundqvist, Phys. Rev. Lett. **95**, 109902(E) (2005).

[15] Y. Gamo, A. Nagashima, M. Wakabayashi, M. Terai, and C. Oshima, Surf. Sci. **374**, 61 (1997).

[16] A. Varykhalov, J. Sánchez-Barriga, A. M. Shikin, C. Biswas, E. Vescovo, A. Rybkin, D. Marchenko, and O. Rader, Phys. Rev. Lett. **101**, 157601 (2008).

[17]D. Eom, D. Prezzi, K. T. Rim, H. Zhou, M. Lefenfeld, S. Xiao, C. Nuckolls, M. S. Hybertsen, T. F. Heinz, and G. W. Flynn, Nano Lett. **9**, 2844 (2009).
[18]J. P. Perdew, K. Burke, and M. Ernzerhof, Phys. Rev. Lett. **77**, 3865 (1996).
[19]S. Grimme, J. Comput. Chem. **27**, 1787 (2006).
[20]G. Kresse and J. Furthmüller, Phys. Rev. B **54**, 11169 (1996).
[21]P. E. Blöchl, Phys. Rev. B **50**, 17953 (1994).
[22]G. Kresse and D. Joubert, Phys. Rev. B **59**, 1758 (1999).
[23]A. Gulans, M. J. Puska, and R. M. Nieminen, Phys. Rev. B **79**, 201105(R) (2009).
[24]M. Amft, S. Lebègue, O. Eriksson, and N. V. Skorodumova, J. Phys.: Condens. Matter **23**, 395001 (2011).
[25]W. R. Tyson and W. A. Miller, Surf. Sci. **62**, 267 (1977).
[26]C. Kittel, *Introduction to Solid State Physics* (Wiley, New York, 1996).
[27]R. F. Bader, *Atoms in Molecules: A Quantum Theory* (Oxford University Press, Oxford, 1990).
[28]G. Henkelman, A. Arnaldsson, and H. Jónsson, Comput. Mater. Sci. **36**, 354 (2006).
[29]E. Sanville, S. D. Kenny, R. Smith, and G. Henkelman, J. Comput. Chem. **28**, 899 (2007).
[30]W. Tang, E. Sanville, and G. Henkelman, J. Phys.: Condens. Matter **21**, 084204 (2009).
[31]K. Toyoda, Y. Nakano, I. Hamada, K. Lee, S. Yanagisawa, and Y. Morikawa, Surf. Sci. **603**, 2912 (2009).
[32]P. Pulay, Chem. Phys. Lett. **73**, 393 (1980).
[33]R. P. Feynman, Phys. Rev. **56**, 340 (1939).
[34]H. Shi and C. Stampfl, Phys. Rev. B **76**, 075327 (2007).
[35]J. Björk, S. Stafström, and F. Hanke, J. Am. Chem. Soc. **133**, 14884 (2011).
[36]D. Syomin, J. Kim, and B. E. Koel, J. Phys. Chem. B **105**, 8387 (2001).
[37]K. Tonigold and A. Gross, J. Chem. Phys. **132**, 224701 (2010).